ACS Chemical Neuroscience

Article

Design, Synthesis, and Structure-Activity-Relationship of Tetrahydropyrido[4,3-d]pyrimidine Derivatives as Potent Smoothened Antagonists with in Vivo Activity

Wenfeng Lu, Yongqiang Liu, Haikuo Ma, Jiyue Zheng, Sheng Tian, Zhijian Sun, Lusong Luo, Jiajun Li, Hongjian Zhang, Zeng-jie Yang, and Xiaohu Zhang

ACS Chem. Neurosci., **Just Accepted Manuscript** • DOI: 10.1021/acschemneuro.7b00153 • Publication Date (Web): 15 Jun 2017

ACS Publications

ACS Chemical Neuroscience is published by the American Chemical Society. 1155 Sixteenth Street N.W., Washington, DC 20036

Design, Synthesis, and Structure-Activity-Relationship of Tetrahydropyrido[4,3-*d*]pyrimidine Derivatives as Potent Smoothened Antagonists with in Vivo Activity

Wenfeng Lu,[†,#] Yongqiang Liu,[‡,#] Haikuo Ma,[†,#] Jiyue Zheng,[†] Sheng Tian,[†] Zhijian Sun,[§] Lusong Luo,*[,§] Jiajun Li,[†] Hongjian Zhang,[†] Zeng-Jie Yang,*[,†,‡] and Xiaohu Zhang*[,†]

[†] Jiangsu Key Laboratory of Translational Research and Therapy for Neuro-Psychiatric-Diseases and College of Pharmaceutical Sciences, Soochow University, Suzhou, Jiangsu 215021, P. R. China

[‡] Cancer Biology Program, Fox Chase Cancer Center, Temple University Health System, Philadelphia, Pennsylvania, USA.

[§] BeiGene (Beijing) Co., Ltd., No. 30 Science Park Road, Zhongguancun Life Science Park, Beijing 102206, P. R. China

Abstract: Medulloblastoma is one of the most prevalent brain tumors in children. Aberrant hedgehog (Hh) pathway signaling is thought to be involved in the initiation and development of medulloblastoma. Vismodegib, the first FDA-approved cancer therapy based on inhibition of aberrant hedgehog signaling, targets smoothened (Smo), a G-protein coupled receptor (GPCR) central to the Hh pathway. Although vismodegib exhibits promising therapeutic efficacy in tumor treatment, concerns have been raised fromits non-linear pharmacokinetic (PK) profiles at high doses partly due to low aqueous solubility. Many patients experience adverse events such as muscle spasms and weight loss. In addition, drug resistance often arises among tumor cells during treatment with vismodegib. There is clearly an urgent need to explore novel Smo antagonists with improved potency and efficacy. Through a scaffold hopping strategy, we have identified a series of novel tetrahydropyrido[4,3-*d*]pyrimidine derivatives, which exhibited effective inhibition of Hh signaling. Among them, compound **24** is three times more

potent than vismodegib in the NIH3T3-GRE-Luc reporter gene assay. Compound **24** has lower melting point and much greater solubility compared with vismodegib, resulting in linear PK profiles when dosed orally at 10, 30, and 100 mg/kg in rats. Furthermore, compound **24** showed excellent PK profiles with a 72% oral bioavailability in beagle dogs. Compound **24** demonstrated overall favorable in vitro safety profiles with respect to CYP isoform and hERG inhibition. Finally, compound **24** led to significant regression of subcutaneous tumor generated by primary Ptch1-deficient medulloblastoma cells in SCID mouse. In conclusion, tetrahydropyrido[4,3-*d*]pyrimidine derivatives represent a novel set of Smo inhibitors that could potentially be utilized to treat medulloblastoma and other Hh pathway related malignancies.

Keywords: medulloblastoma, hedgehog signaling pathway, Smoothened, antagonist, GPCR, scaffold hopping, cancer therapy

INTRODUCTION

Medulloblastoma is one of the most prevalent brain tumors in children. Aberrant hedgehog (Hh) pathway signaling is thought to be involved in the initiation and development of medulloblastoma.[1,2] The hedgehog (Hh) signaling pathway is a pivotal developmental pathway which is responsible for cell growth, patterning, and migration during embryogenesis. Its function is, however, limited to tissue maintenance and stem cell regulation in adults. Ordinarily, the secreted proteins Sonic hedgehog, Indian hedgehog and Desert hedgehog bind to their cellular membrane receptor Patched (Ptch), relieving the suppression of Ptch to Smoothened (Smo), a G protein coupled receptor. Activated Smo then triggers a series of intracellular events which involve the glioma-associated oncogene transcription factors' (Gli1, Gli2, and Gli3) dissociation from suppressor of fused (SUFU) and translocation to the nucleus to transcribe Hedgehog target genes.[3,4] Over activation of Hh signaling has been implicated in multiple human malignancies. Ligand-independent activation of the Hh signaling pathway caused by mutational inactivation of the inhibitory pathway components e.g. Ptch (lost-of-function of Ptch) or activation of Smo (gain-of-function of Smo) leads to medulloblastoma and basal cell carcinoma.[5,6] Ligand-dependent activation of Hh signaling is observed in colorectal, pancreatic, lung, prostate and blood cancers.[7-9] Therefore, mitigation of hyperactivation of Hh signaling represents an attractive therapeutic strategy for cancer treatments.[10-15]

The first Hh signaling pathway inhibitor reported in the literature was cyclopamine (Figure 1), a naturally occurring alkaloid later identified as a Smo inhibitor.[16] IPI-926 (Figure 1) was then developed based on the framework of cyclopamine. IPI-926 exhibited not only better chemical stability and potency, but also much improved metabolic stability, pharmacokinetic profiles and other superior pharmaceutical properties than those of cyclopamine.[17-19] Infinity Pharmaceuticals initiated clinical

trials with IPI-926. Unfortunately, all clinical development efforts were suspended following disappointing results of a phase II study of IPI-926 in patients with metastatic chondrosarcoma.[20] More encouragingly, NVP-LDE225, a synthetic small molecule Smo inhibitor, demonstrated promising results in clinical development for advanced basal cell carcinoma.[21,22] The mixed results underscored the complex nature of Hh signaling and prompted debate over whether blockage of ligand dependent Hh pathway activation could be effective in cancer therapy.[14,15] Despite the uncertainty, many Smo inhibitors have been developed in recent years (Figure 1).[23-37] In January 2012, vismodegib (GDC-0449, Figure 1) was approved by FDA for patients with locally advanced or metastatic basal cell carcinoma which was not suitable for operation.[38] This approval highlights the first-in-class small molecule Smo antagonist for the treatment of human cancer and validated decades of basic research in hedgehog signaling pathway. However, vismodegib suffered from suboptimal physicochemical properties such as low aqueous solubility, resulting in non-linear pharmacokinetic profiles at high doses. Adverse events such as muscle spasms and weight loss occurred in many patients. In addition, vismodegib suffered from resistance in patients.[39-41] Accumulating evidence suggests that Smo antagonists with diverse structures, even though binding to the same site as vismodegib, may be capable of blocking the mutant Smo.[20,25-27] This effect may be due to the extended interactions between Smo and the antagonists away from the mutant site. Therefore, Smo inhibitors with diverse chemical structures and improved potency and efficacy may be able to address the needs of patients who do not benefit from vismodegib. In July 2015, a second Smo inhibitor, sonidegib (NVP-LDE225, Figure 1), was approved by FDA for the treatment of locally advanced basal cell carcinoma.[42] This new approval highlights the continued efforts and interests in research and development of hedgehog pathway inhibitors. Here we report our work on a series of Smo antagonists based on a novel tetrahydropyrido[4,3-*d*]pyrimidine template.

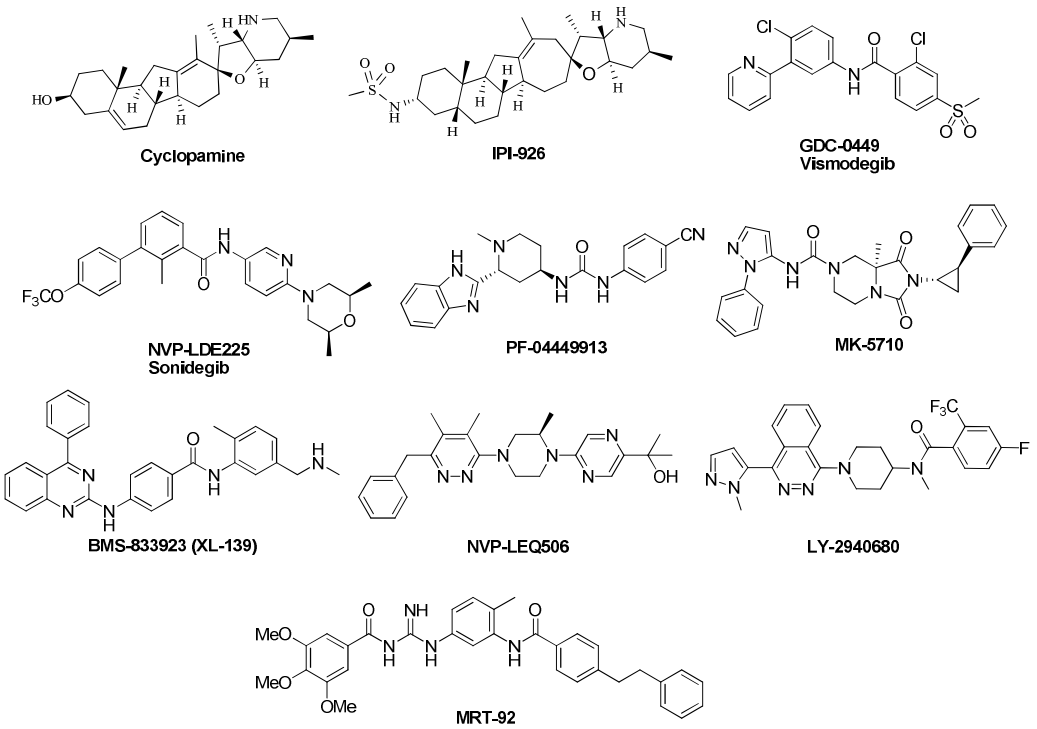

Figure 1. Structures of advanced smoothened antagonists reported in the literature

RESULTS AND DISCUSSION

Compound Design Rationale. In our effort to pursue novel Smo inhibitors, we explored numerous templates with the guidance of the recently solved Smo crystal structures[43-47] and a pharmacological model.[34] Vismodegib (GDC-0449)[25] was obtained by optimization campaign originated from high-throughput screening hits. With the exception of the terminal methyl group, the skeleton of vismodegib was constructed uniformly with sp^2-hybridized carbons, resulting in a very high melting point (264 °C) and poor solubility (9.5 μg/mL). In the process of optimizing vismodegib, the ortho-chloro group was added to the right side ring to introduce tilt and reduce planarity of the aryl amide, despite adding additional molecular weight and clogP, to improve its solubility.[25] In clinical development, vismodegib was hampered by its non-linear pharmacokinetic profiles at high doses, most likely due to its high crystal packing energy and poor aqueous solubility. We have encountered a similar problem in an adenosine antagonist program before.[48,49] Molecular topology and planarity have

significant impact on physicochemical properties such as solubility is well documented in the literature.[50,51] In an attempt to improve the physicochemical properties of our designed compounds, we proposed to introduce sp^3-hybridized saturation ring as a place-holder, as featured in SEN794[32] and PF-5274857[52], as a way to reduce planarity. We also proposed forming a ring on the tail part in SEN794 and PF-5274857 to decrease rotatable bonds, as a way of enhancing metabolic stability and absorption.[53] We applied this strategy to obtain a number of novel scaffolds exemplified by tetrahydroimidazo[1,2-*a*]pyrazine,[54] tetrahydrothiazolo[5,4-*c*]pyridine,[55] and tetrahydropyrido[4,3-*d*]pyrimidine, as shown in Figure 2. We initially worked on tetrahydroimidazo[1,2-*a*]pyrazine scaffold based on its low clogP (2.4) and polar surface area (73). The pKa (7.5) is also attractive because it may further improve the solubility of its derivatives, without overtly changing their ionization stage. Unfortunately, the best compounds we could optimize from the tetrahydroimidazo[1,2-*a*]pyrazine scaffold were at least 5 times less potent compared with vismodegib in our screening assay.[54] Better results were achieved from optimization of the tetrahydrothiazolo[5,4-*c*]pyridine scaffold. We were able to obtain compounds as potent as vismodegib. In addition, the leading compounds also showed good pharmacokinetic profiles and improved solubility. Encouraged, we decided to also work on the tetrahydropyrido[4,3-*d*]pyrimidine scaffold, because the pyrimidine is a closer bioisostere to thiazole in size and the template has a much lower intrinsic clogP (2.9, Figure 2). The crystal complex of vismodegib interacts with Smo receptor was released (PDB ID: 5L7I) recently by Byrne et al.[43] Based on this work, we examined the interaction patterns between compounds **12** and **16** (Table 1) generated from Template III (Figure 2) and Smo receptor by using SP (standard precision) and XP (extra precision) scoring functions in *Glide*.[56] The detailed docking procedure has been reported in our previous study.[57] According to *Glide* docking results, the predicted

binding affinities of compound **12** was worse than, while compound **16** was better than that of vismodegib against Smo receptor evaluated by the docking scores. For example, the docking scores of compounds **12**, **16**, and vismodegib were -5.951, -9.491, and -7.828 by using SP scoring mode of *Glide*, respectively. Similar results were observed in *Glide* XP scoring function studies. The computational predictions indicated that promising Smo receptor antagonists may be obtained based on Template III. In addition, we also found that the binding poses of compounds **12** and **16** predicted by *Glide* docking were quite similar to that of the vismodegib. It demonstrated that the key interactions derived from the vismodegib-Smo crystal complex were almost reserved by our scaffold optimizations. The docking poses of compounds **12** and **16** from *Glide* SP docking were depicted in Figure 3 using DS2.5.[58] Here we report the results from the exploration of the tetrahydropyrido[4,3-*d*]pyrimidine template.

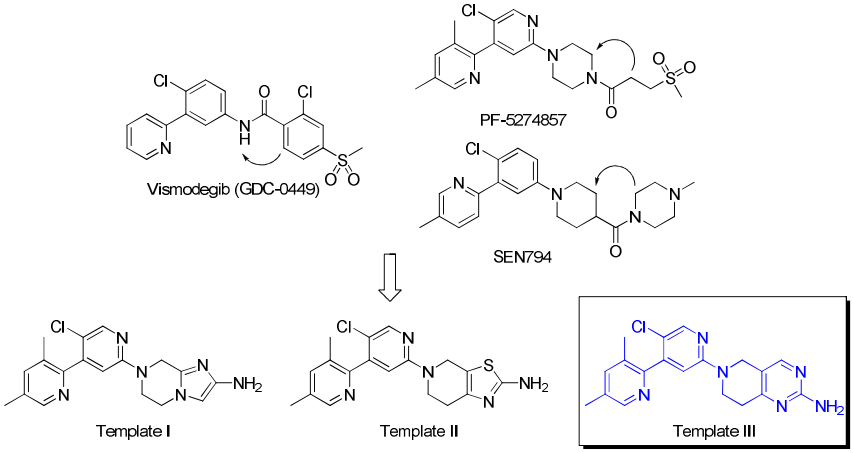

	Template I	Template II	Template III
clogP	2.4	3.9	2.9
PSA	73	68	81
pKa	7.5	5.8	4.1

Figure 2. Design rationale of new templates

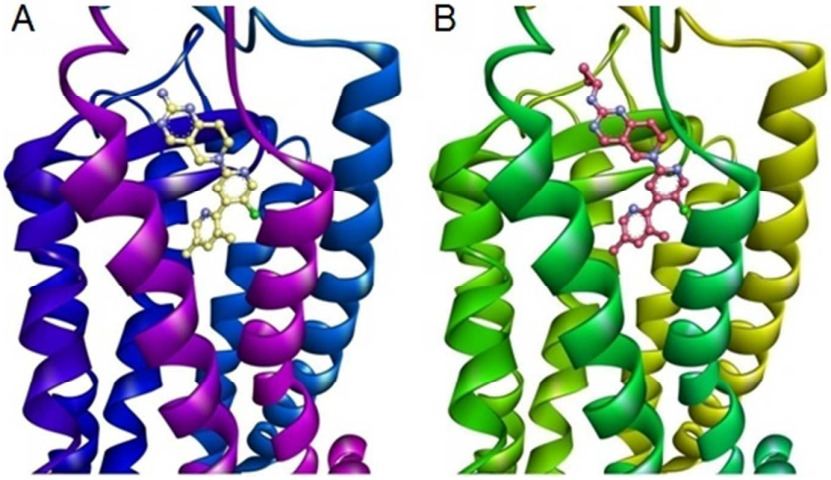

Figure 3. The docking poses of compounds **12** (A) and **16** (B) derived from *Glide* SP docking in Smo receptor.

Chemistry. The synthesis of compounds **12-16**, **20**, **21**, **26**, **27**, and **32-34** was undertaken as outlined in Scheme **1**. The commercial available 2,5-dichloropyridine **1** was treated with LDA and then triisopropyl borate to afford boronic acid **2**.[59] The key intermediate **3** was obtained by Suzuki coupling of **2** with 2-bromo-3,5-dimethyl-pyridine in the presence of Pd(dppf)Cl_2 and K_3PO_4•$3H_2O$. A two-step sequence involving piperidone **4** treated with DMF-DMA in reflux followed by ring closure with *S*-methylisothiourea sulfate and sodium acetate gave tetrahydropyrido[4,3-*d*]pyrimidine **5**. Oxidization of intermediate **5** with *m*-CPBA provided sulfone **6**. The intermediate **6** was substituted with corresponding amines toafford intermediates **7a-k**. Removal of the Boc of **7a-k** with HCl afforded amines **8a-k**, which were reacted with **3** in the presence of CsF to give compounds **12-16**, **20**, **21**, **26**, **27**, **32**, and **33**. Sulfonylation of **13** with methyl sulfonyl chloride gave compound **34**.

Scheme 1.Synthesis of Analogues**12-16**, **20**, **21**, **26**, **27**,and **32-34**

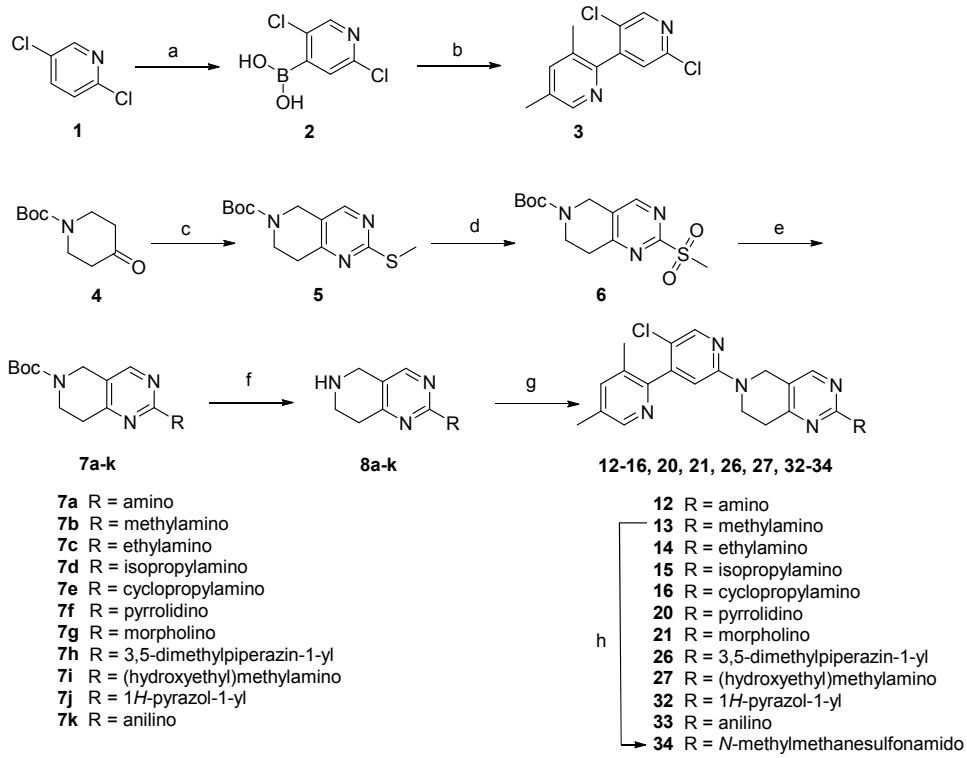

[a]Reagents and conditions: (a) LDA, THF, -78 °C, 1 h, then triisopropyl borate, THF, rt, 2 h; (b) 2-bromo-3,5-dimethyl-pyridine, Pd(dppf)Cl_2, K_3PO_4•$3H_2O$, dioxane/H_2O, 110 °C, 12 h; (c) i) DMF-DMA, 100 °C, 12 h; ii) *S*-methylisothiourea sulfate, EtONa, EtOH, 80 °C, 12 h; (d) *m*-CPBA, CH_2Cl_2, 0 °C to rt, 12 h; (e) corresponding amines, *t*-BuOH, 90 °C,16 h for **7a-i**; NaH, pyrazole, THF, 0 °C, 1 h for **7j**; aniline, 100 °C, 48 h for **7k**; (f) HCl/EtOAc, rt, 5 h; (j) **3**, CsF, DMSO, 120 °C, 36 h; (h) MsCl, TEA, CH_2Cl_2, 0 °C, 3 h.

Compounds **17-19**, **22-25** and **28-31** were prepared as shown in Scheme **2**. Removal of the Boc of intermediate **5** with HCl afforded amine **9**, which was reacted with **3** in the presence of CsF to give intermediate **10**. Intermediate **10** was oxidized with oxone, then displaced with corresponding amines or alcohols to yield compounds **17-19**, **22-25**, and **28-31**.

Scheme 2. Synthesis of Analogues**17-19**, **22-25**, and **28-31**[a]

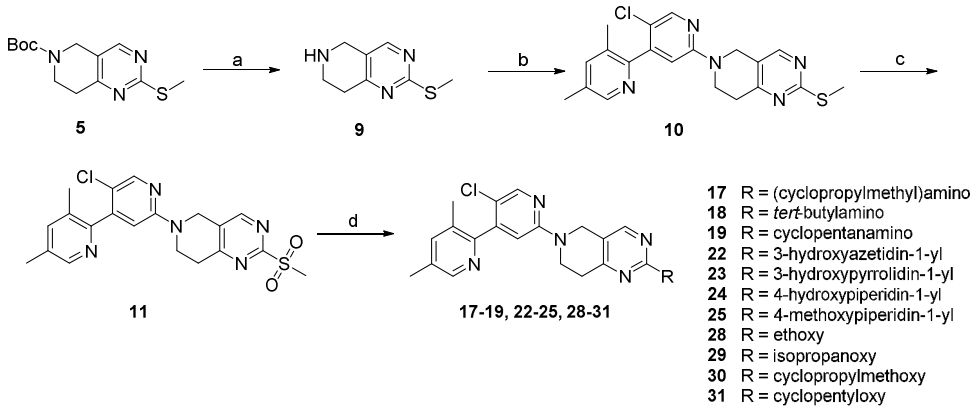

[a]Reagents and conditions: (a) HCl/EtOAc, rt, 5 h; (b) **3**, CsF, DMSO, 120 °C, 36 h; (c) oxone, THF, rt, 12 h; (d) corresponding amines, *t*-BuOH, 80 °C, 12-72 h for **17-19**, **22-25**; EtONa, EtOH, 0 °C, 1 h for **28**; NaH, *i*-PrOH, 0 °C, 2 h for **29**; corresponding alcohols, NaH, THF, 0 °C, 3 h for **30** and **31**.

The biheteroaryl halides **37a-i**, **48a**, and **48b** were obtained through either Negishi coupling or Suzuki coupling (Schemes 3 and 4). The 2-chloride of intermediates **37a-i**, **48a**, and **48b** were substituted with amine **8e** to give the compounds **38-46**, **49**, and **50**.

Scheme 3. Synthesis of Analogues **38-46**[a]

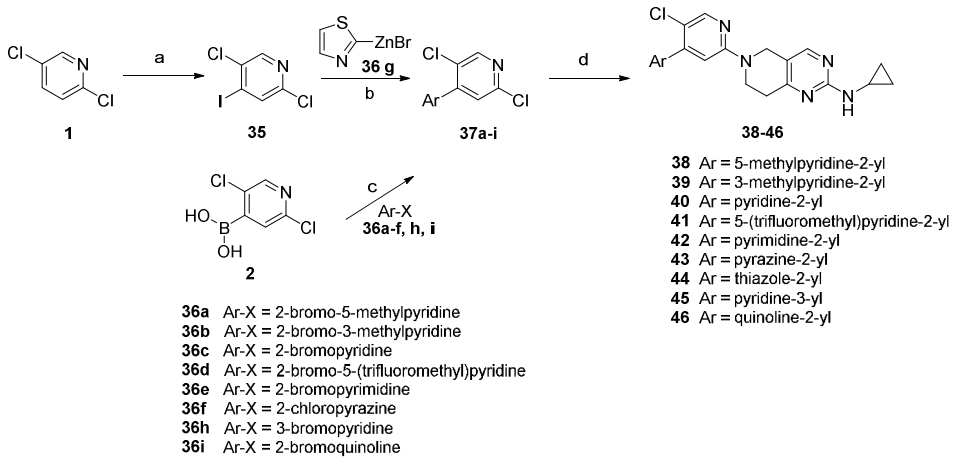

[a]Reagents and conditions: (a) *n*-BuLi, THF, -60 °C, 2 h, then iodine, THF, -60 °C, 2 h; (b) $Pd(PPh_3)_4$, THF, reflux, 12 h; (c) $K_3PO_4 \cdot 3H_2O$, $Pd(dppf)Cl_2$, dioxane/H_2O, 110 °C, 12 h for **37a** and **37b**; Na_2CO_3, $Pd(dppf)Cl_2$, DME/H_2O, 100 °C, 16 h for **37c** and **37h**; $K_3PO_4 \cdot 3H_2O$, $Pd(dppf)Cl_2$, THF/H_2O, 60 °C, 16 h for **37d**; 2 N K_2CO_3, $Pd(PPh_3)_4$, EtOH/toluene, 115 °C, 16 h for **37e** and **37i**; Na_2CO_3, $Pd(PPh_3)_4$,

dioxane/H_2O, 130 °C, 16 h for **37f**; (d) **8e**, CsF, DMSO, 120 °C, 36 h.

Scheme 4. Synthesis of Analogues **49** and **50**[a]

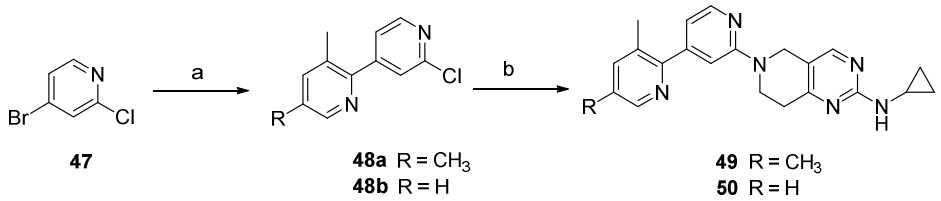

[a]Reagents and conditions: (a) bis(pinacolato)diboron, AcOK, Pd(dppf)Cl_2, dioxane, 110 °C, 6 h, then 2-bromo-3,5-dimethylpyridine or 2-bromo-3-methylpyridine, K_3PO_4•$3H_2O$, dioxane/H_2O, 110 °C, 8 h; (b) **8e**, LiCl, K_2CO_3, DMSO, 140 °C, 36 h.

Compound **55** was prepared according to Scheme 5. Treatment of 2-bromo-3,5-dimethyl-pyridine **51** with *n*-BuLi and then *N,N*-dimethylpropionamide to provide ketone **52**. Reaction of **52** with DMF-DMA and followed by cyclization with *S*-methylisothiourea sulfate provided thioether **53**. Oxidation of the thioether group of **53** with oxone afforded sulfone **54**, which was substituted with **8e** to give final compound **55**.

Scheme 5. Synthesis of Compound **55**[a]

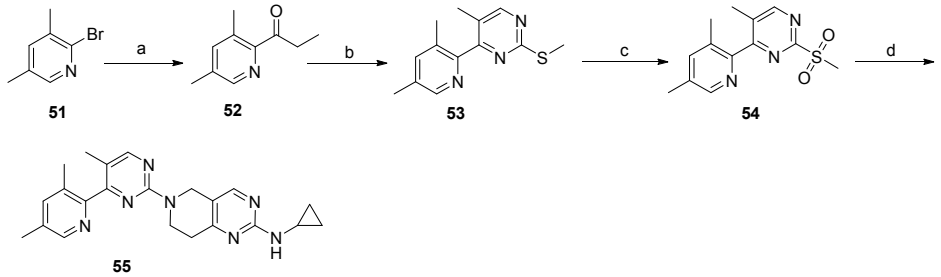

[a]Reagents and conditions: (a) *n*-BuLi, THF, -78 °C, 10 min, then *N,N*-dimethylpropionamide, THF, -78 °C, 1 h; (b) (i) DMF-DMA, 80 °C, 12 h; (ii) *S*-methylisothiourea sulfate, EtONa, EtOH, reflux, 12 h; (c) oxone, THF, 0 °C to rt, 16 h; (d) **8e**, DIPEA, *t*-BuOH, reflux, 24 h.

Compounds **63** and **64** were prepared as outlined in Scheme **6**. Aniline **58** was prepared from the

commercial available **56** in two steps via diazotization followed by reduction. Aniline **58** was converted to borate ester **59** and then coupled with 2-bromo-3,5-dimethyl-pyridine or 2-bromopyridine to give intermediates **60a** and **60b**, respectively. Iodine was introduced by diazotization-iodination to give **61a** and **61b**. Buchwald coupling of amine **9** with **61a** or **61b** were carried outin the presence of $Pd(dba)_2$ and XPhos to afford **62a** and **62b**, respectively. The thioether group of **62a** and **62b** was oxidized using sodium perborate, and then displaced with cyclopropylamine to give compounds **63** and **64**, respectively.

Scheme 6. Synthesis of Analogues **63** and **64**[a]

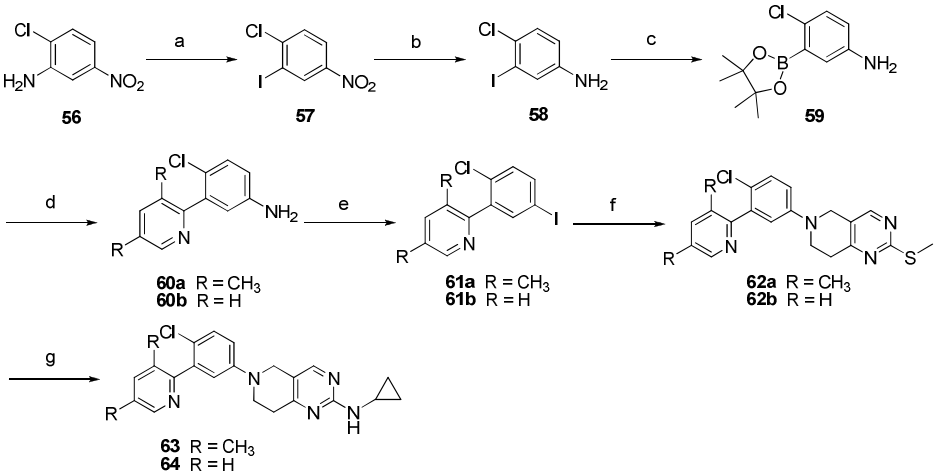

[a]Reagents and conditions: (a) $NaNO_2$, HCl, H_2O, 0 °C, 0.5 h, then KI, H_2O, 0 °C to rt, 0.5 h; (b) Fe, NH_4Cl, EtOH/H_2O, 75 °C, 3 h; (c) bis(pinacolato)diboron, $Pd(dppf)Cl_2$, AcOK, DMF, 120 °C, 2.5 h; (d) **51** or 2-bromopyridine, K_3PO_4•$3H_2O$, $Pd(PPh_3)_4$, dioxane/H_2O, 110 °C, 12 h; (e) $NaNO_2$, HCl, H_2O, 0 °C, 1 h, then KI, H_2O, 0 °C to rt, 1 h; (f) **9**, $Pd(dba)_2$, XPhos, Cs_2CO_3, dioxane, 110 °C, 12 h; (g) (i) $NaBO_3$•$4H_2O$, MeCN, rt, 16 h; (ii) cyclopropylamine, *t*-BuOH, 90 °C, 48 h.

Evaluation of Pharmacological Activity and Structure Activity Relationship. We have developed two assays to characterize the synthesized compounds. The detailed experimental procedures were reported before.[54,55,60] Briefly, the primary screening assay was a cell based NIH3T3-GRE-Luc reporter

gene assay with 10 nM SAG as the Hh pathway agonist.[23,61,62] This assay is suitable to identify Smo antagonists and Gli inhibitors but is not applicable to identify compounds interacting with targets upstream of Smo, such as hedgehog protein inhibitors[63], or hedgehog acyltransferase inhibitors[64]. In order to confirm that the synthetic compounds were interacting with Smo, we developed a competitive displacement assay based on fluorescence signal. In this assay, the synthesized compounds were evaluated for their ability to displace BODIPY-cyclopamine in the U2OS cells over-expressing human Smo.[16,65,66]

The structure-activity-relationship is summarized in Tables 1 and 2.

Table 1. SAR of the right-hand side structural elements

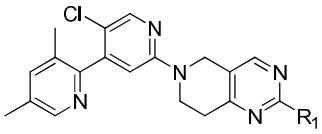

Compd	R_1	N-G-L IC_{50} (nM) ± SEM[a]	SMO-BCB IC_{50} (nM) ± SEM[b]	Compd	R_1	N-G-L IC_{50} (nM) ± SEM[a]	SMO-BCB IC_{50} (nM) ± SEM[b]
12		>1000		**24**	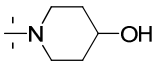	7.5 ± 2.4	24 ± 2.5
13		330 ± 97		**25**	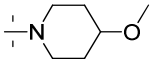	110 ± 24	71 ± 1.0
14		27 ± 11		**26**	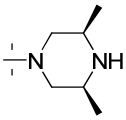	14 ± 2.7	
15		28 ± 11		**27**	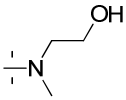	46 ± 23	
16		15 ± 10	41 ± 12	**28**		150 ± 52	
17	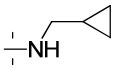	58 ± 27	41 ± 9.0	**29**		70 ± 28	

18		19 ± 5.3	**30**	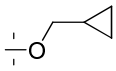	63 ± 21	
19	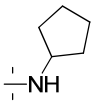	76 ± 42	**31**	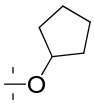	54 ± 23	
20		36 ± 11	**32**		98 ± 50	
21	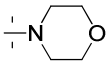	66 ± 17	**33**	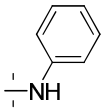	56 ± 53	
22	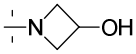	240 ± 40	**34**		100 ± 44	
23	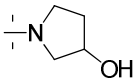	56 ± 29		**Vismodegib** [c]	21 ± 12	92 ± 13

[a] Inhibition of luminescence signaling in NIH3T3-GRE-Luc reporter gene assay (N-G-L) with 10 nM SAG as the Hh pathway agonist. Data are expressed as geometric mean values of at least two runs ± the standard error measurement (SEM).

[b] Inhibition of BODIPY-cyclopamine fluorescence signaling in the competitive displacement experiment using U2OS cells over-express human SMO. Data are expressed from a single IC_{50} determination.

c Vismodegib was run as standard in each assay. Data are expressed as geometric mean values of six runs ± the standard error measurement (SEM).

Table2. SAR of the left-hand side structural elements

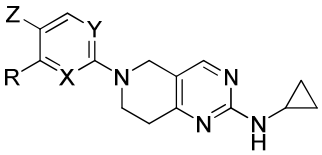

Compd	R	X	Y	Z	N-G-L IC_{50} (nM) ± SEM[a]
38	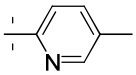	CH	N	Cl	350 ± 43

39	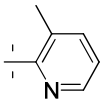	CH	N	Cl	67 ± 16
40	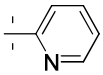	CH	N	Cl	400 ± 70
41	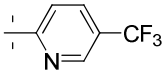	CH	N	Cl	550 ± 140
42	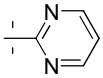	CH	N	Cl	>1000
43	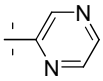	CH	N	Cl	330 ± 99
44		CH	N	Cl	190 ± 52
45	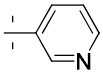	CH	N	Cl	650 ± 340
46	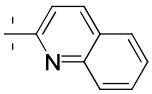	CH	N	Cl	96 ± 16
49	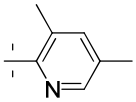	CH	N	H	74 ± 19
50	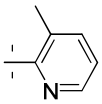	CH	N	H	54 ± 6
55	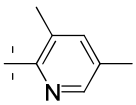	N	N	CH_3	450 ± 150
63	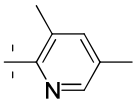	CH	CH	Cl	11 ± 8.5
64	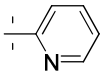	CH	CH	Cl	110 ± 16
	Vismodegib[b]				21 ± 12

[a] Inhibition of luminescence signaling in NIH3T3-GRE-Luc reporter gene assay (N-G-L) with 10 nM SAG as the Hh pathway agonist. Data are expressed as geometric mean values of at least two runs ± the standard error measurement (SEM).

[b] Vismodegib was run as standard in each assay. Data are expressed as geometric mean values of six

runs ± the standard error measurement (SEM).

The simplest compound of this series of analogues was inactive (compound **12**, >1000 nM). Addition of a methyl group on the right-hand side terminal nitrogen effectively brought down activity to 330 nM. The trend continued as ethyl, isopropyl, *t*-butyl quickly brought activity down to low nano-molar range (compounds **14**, **15**, **18**; 27, 28, and 19 nM, respectively). Compound **18** was as potent as vismodegib (21 nM) in the same assay. Cyclization of the alkyl groups was well tolerated, as demonstrated by compounds **16**, **17**, and **19** (15, 58, and 76 nM, respectively). Compound **16** was slightly more active compared with vismodegib. Secondary amines, either with cyclic structures (compounds **20-25**) or acyclic structure (compound **27**), were well tolerated. Among them, compound **24** was three times more potent than vismodegib. We also incorporated ether linkage (compounds **28-31**) and aromatic elements (compounds **32** and **33**) to the terminal nitrogen, without significantly improving potency. Finally, sulfonamide **34** (100 nM) was synthesized, but it was five times less potent compared with vismodegib. The overall SAR trend largely followed the tetrahydrothiazolo[5,4-*c*]pyridine series.[55]

Having established the SAR on the right-hand side region of this scaffold, we turned our focus on the optimization of the left-hand side bi-aryl region of this template. To do so, cyclopropyl amine was arbitrarily fixed on the right-hand side (Table 2). Removal of the ortho-methyl group on the left-hand terminal 2-pyridine ring led to significant potency loss (compound **38**, 350 nM). This was in contrast to the moderate potency loss when the para-methyl group was removed (compound **39**, 67 nM). Potency was almost unchanged when both methyl groups were removed (compound **40**, 400 nM). This observation indicated that the bi-aryl group might need to be tilted to ensure a better fit or interaction with the smoothened receptor. This is in consistence with the crystal structure and molecular modeling. Replacement of the para-methyl with a trifluoromethyl slightly reduced potency. Introduction of an

additional nitrogen to the terminal pyridine ring led to very different results: while 2,5-pyrazine was tolerated, 2,6-pyrimidine led to totally inactive compound (compounds **43**, **42**; 330, >1000 nM, respectively). As a bioisostere of 2-pyridine, 2-thiazole was active (compound **44**, 190 nM). We were unable to improve potency either by moving the nitrogen around the ring (compound **45**, 650 nM), or by adding an extra ring (compound **46**, 96 nM) to the scaffold. Overall, the initial 4,6-dimethyl 2–pyridine remained the best structural element after the SAR study. We then focused our optimization on the internal ring of the left-hand side bi-aryl element. Removal of the chlorine led to moderate reduction of potency (compound **49**, 74 nM). Replacement of the chloro pyridine with methyl pyrimidine led to over twenty folds potency loss (compound **55**, 450 nM), while introduction of chloro phenyl ring improved the potency slightly (compound **63**, 11 nM). This improvement was maintained when the terminal aryl ring was replaced by 2-pyridine, as compound **64** was four times more potent compared with compound **40** (110 nM vs. 400 nM). Although compound **63** was twice as potent as vismodegib, given the unfavorably high clogP (clogP of **63**, 4.8 vs. clogP of **16**, 4.1), the chloro phenyl element was de-prioritized. In summary, through a scaffold hopping strategy, we obtained a novel tetrahydropyrido[4,3-*d*]pyrimidine template which provided compounds with hedgehog inhibition activity more potent than vismodegib (e.g. compounds **24** and **63**) evaluated by the reporter gene assay. We were able to identify the preferred structural pieces on the right-hand side and on the left-hand side after the initial SAR study. Compounds **16** and **24** were identified as early leads. Although compound **16** was as potent as vismodegib in our primary screening assay, it exhibited a number of potential problems that warranted to be monitored closely: it showed moderate CYP inhibition at10 μM concentration (Table 4). Furthermore, the cyclopropyl amine structural element had been linked to reactive metabolites in numerous cases which might lead to toxicity.[67,68] Conversely, compound **24**

showed no significant inhibition to multiple CYP isoforms, suggesting a more favorable drug-drug interaction profile.

The reporter gene assay can effectively identify active compounds downstream of smoothened and is suitable for high through screening. However, as compounds with common cell toxicity can also inhibit the reporter gene and therefore cause false positive results, we used a Wnt pathway reporter gene assay as a counter screening assay to minimize the possibility for false positive results.[69,70] Nonspecific cell toxicity was confirmed not to be the source of hedgehog inhibition activity (data not shown). Finally, we used a fluorescence-based competitive displacement assay to confirm that the new compounds were indeed Smo antagonists. Compounds **16** and **24** effectively displaced BODIPY-cyclopamine in the U2OS cells over-expressing human Smo (41 and 24 nM, respectively. vismodegib was less active in this assay at 92 nM, Table 1), validating Smo as their molecular target.

Evaluation of Physicochemical Properties. By designing the novel scaffold, we aimed to maintain the excellent potency inherent from the known templates while fostering improved physicochemical properties (e.g. solubility). As a way to achieve this goal, we introduced sp^3-hybridized carbons, thus reducing planarity and disrupting crystal packing, in hope to lower the melting point and improve solubility. The solubility and melting point of compounds **16** and **24** from the tetrohydrothiazolopyridine scaffold along with vismodegib were determined in the same assay conditions and the results were summarized in Table 3 (the data reported in the literature was also included for comparison). We selected these two compounds to compare with vismodegib because these two compounds were equally or more potent compared with vismodegib (Table 1). In addition, these compounds had similar clogP to vismodegib (Table 3). Under the current experimental conditions, vismodegib demonstrated a solubility of 4.1 μg/mL at pH 6.5, while compounds **16** and **24**

demonstrated a much improved solubility of 2770 μg/mL and 90 μg/mL, respectively, at pH 6.5. Furthermore, the melting point of compounds **16** and **24** was determined to be 60 °C lower than that of vismodegib (Table 3), suggesting that the added sp^3-hybridized carbons indeed lowered the crystal lattice energy.

Table 3. Solubility and melting point of leading compounds

Compd	clogP[a]	Melting point (°C)[b]	Solubility (μg/mL)[c]	
			pH = 1.0	pH = 6.5
16	4.1	154	>70000	2770
24	3.1	187	>6000	90
Vismodegib	3.6	250	3150 ± 90	4.1 ± 0.5
	4.0[d]	264[d]	>3000[d]	9.5[d]

[a] Calculated by Molinspiration. [b]All compounds were tested as crystalline HCl salts. [c]All compounds were tested as crystalline HCl salts. Data are measured three times ± the standard error measurement (SEM). [d] Reported in the literature.[25]

Evaluation of in Vitro Safety. Compounds **16** and **24** were evaluated in a CYP screening assay in order to assess their drug-drug interaction potentials and liver safety. Compound **16** exhibited moderate inhibition of CYP3A4, 1A2, 2C9, and 2C19 at 10 μM. In contrast, compound **24** showed minimal inhibition of all CYP isoforms tested at the same concentration, suggesting low drug-drug interaction liability. This may partly due to the relatively lower clogP value of compound **24**. Compound **24** was further profiled by a standard patch clamp (express) experiment for its inhibition of the human ether-a-go-go related gene (hERG) potassium channel. Compound **24** exhibited very low inhibition (IC_{50} = 38 μM) of hERG, indicating minimal cardiotoxicity liability associated with blockade of this

key potassium channel. Compound **24** was found to be highly permeable (33× 10^{-6} cm/s, Caco-2), and not likely to be a substrate for efflux (Table 4).

Table 4. In vitro safety data of **16** and **24**

Compd	clogP [a]	CYP Inhibition (%) [b]					hERG (μM)	Caco-2	
		3A4	2D6	1A2	2C9	2C19		P_{app}(A-B) (10^{-6} cm/s)	efflux ratio (B-A)/(A-B)
16	4.1	60	27	76	69	70			
24	3.1	8.0	21	49	30	33	38	33	0.53
Vismodegib	4.0	2.7	24	81	51	44			

[a] Calculated by Molinspiration. [b] All compounds were tested at 10 μM concentration.

Evaluation of Pharmacokinetic Properties and *in Vivo* Safety. Encouraged by the overall satisfactory potency and in vitro safety data,we decided to assess the *in vivo* pharmacokinetic profile of compound **24**. When dosed orally in male Sprague-Dawley (SD) rats, compound **24** exhibited a T_{max} of 0.5 h and a C_{max} of 2180 ng/mL. Compound **24** displayed a moderate clearance (18.6 mL/min/kg), a good steady state volume of 1.7 L/kg, and a half-life of 2.3 h. The oral exposure of compound **24** yielded an AUC of 5541 ng·h/mL, leading to an estimated oral bioavailability of 62% (Table 5). Further, compound **24** demonstrated a proportional PK profile when the oral doses were increased to 30 and 100 mg/kg (Table 5). The enhanced oral exposure of compound **24** at 30 and 100 mg/kg validated the initial goal to improve physicochemical property as a way to improve drug exposure at higher doses. Compound **24** can cross the blood brain barrier with an exposure of 831 ng/g at one hour after oral dosing of 10 mg/kg, resulting in a brain/plasma ratio of 0.4. Given the tumor inhibition efficacy models are mostly carried out in mouse, the PK of compound **24** was also determined in ICR mouse. After oral dosing (10 mg/kg), compound **24** exhibited a T_{max} of 0.25 h and a C_{max} of 4132 ng/mL. Compound **24**

displayed a moderate clearance (20 mL/min/kg), a good steady state volume of 1.0 L/kg, and a half-life of 1.0 h. The oral exposure of compound **24** was at an AUC of 4183 ng·h/mL, resulting in an estimated bioavailability of 49% (Table 5). Based on the encouraging rodent PK data, compound **24** was further tested in Beagle dogs. When dosed orally at 5 mg/kg, compound **24** exhibited a T_{max} of 1 h and a C_{max} of 1300 ng/mL. Compound **24** displayed a moderate clearance (8.1 mL/min/kg), a good steady state volume of 1.8 L/kg, and a half-life of 5.4 h. The oral exposure of compound **24** was excellent with an AUC of 7656 ng·h/mL, resulting in an estimated bioavailability of 72% in beagle dogs (Table 5). Pharmacokinetic evaluation in rodents and dogs indicated that compound **24** had the potential to mitigate the solubility-limited PK seen in vismodegib.

Table 5. Pharmacokinetic data of **24**

Compd	species	route	Dose (mg/kg)	AUC_{0-24h} (ng·h/mL)	CL (mL/min/kg)	$V_{d,ss}$ (L/kg)	C_{max} (ng/mL)	T_{max} (h)	$t_{1/2}$ (h)	F%
24	Mouse	i.v.	2	1701	20	1.0			1.2	
		p.o.	10	4183			4132	0.25	1.0	49
	Rat	i.v.	2	1780	18.6	1.7				
		p.o.	10	5541			2180	0.5	2.3	62
			30	41900			8150	1	2.4	
			100	251000			18400	1	2.6	
	Dog	i.v.	1	2062	8.1	1.8			2.2	
		p.o.	5	7656			1300	1	5.4	72

Based on the aforementioned data, compound **24** was evaluated in a dose escalating toxicity study in mouse (Figure 4). The compound was well tolerated at all doses (100, 250, and 500 mg/kg,

daily oral gavage) and all animal exhibited normal behavior and consumed normal amount of food in the 14-day observation period. Slight increase of liver weight was observed at 250 and 500 mg/kg, and no adverse effects were observed in other organs. The exposure of **24** after 2 h at 100 mg/kg was 22200 ng/mL and 32300 ng/mL on day 1 and day 14, respectively, indicating no significant CYP induction or compound accumulation had occurred.

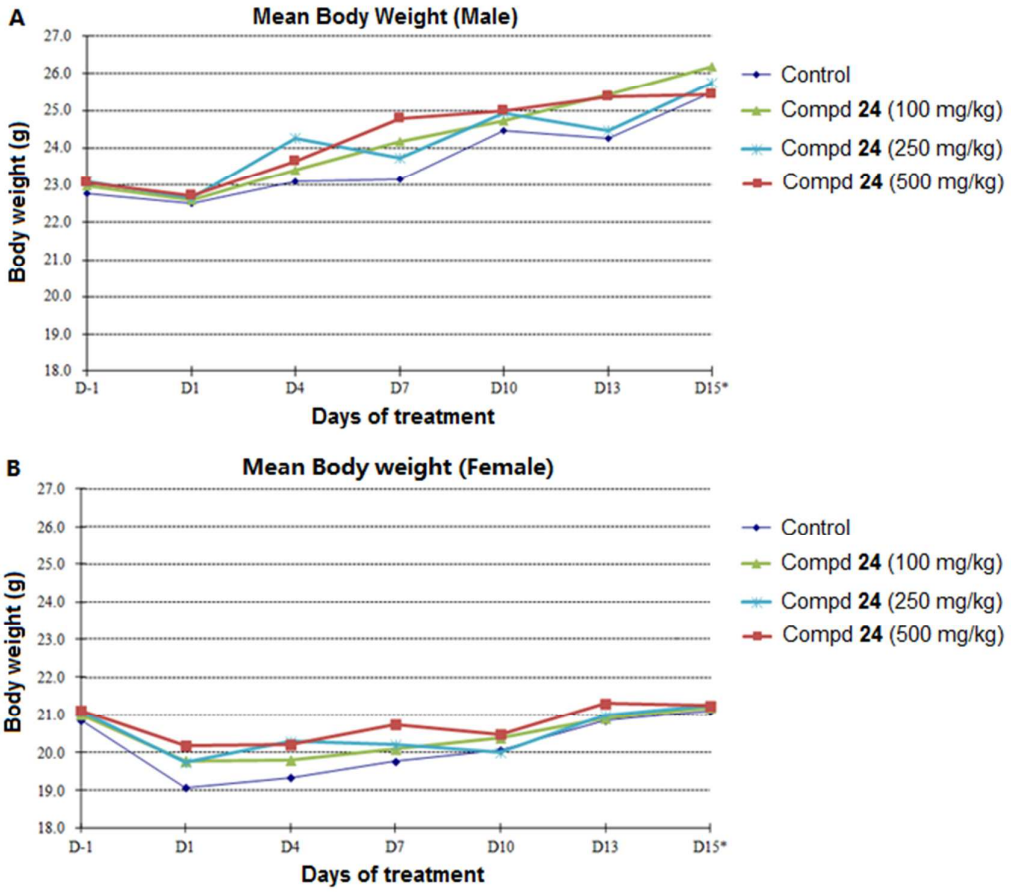

Figure 4. The mean body weight of male (n = 5) and female (n = 5) ICR mouse after receiving 100, 250, and 500 mg/kg compound **24**by daily oral gavage in the 14-day observation period.

Evaluation of In Vivo Efficacy. We next tested the capacity of compound **24** in inhibiting tumor growth by utilizing a subcutaneous xenograft model of *Ptch1*$^{+/-}$ mouse medulloblastoma.[71,72] Tumor cells were freshly isolated from medulloblastoma formed in *Ptch1*$^{+/-}$ mice, in which one allele of Ptch1 gene is mutant. 15-20% of *Ptch1*$^{+/-}$ mice develop medulloblastoma in their cerebella at

around 30 weeks of age. The procedure of isolating tumor cells was previously described.[73] In brief, tumor tissue was enzymatically digested in a papain solution for 30 minutes to obtain a single-cell suspension, which was then centrifuged through a 35% and 65% Percoll gradient. Cells from the 35% to 65% interface were harvested and suspended in Dulbecco's PBS plus 0.5% BSA. The above procedure yields a cell suspension enriched with tumor cells (>95%). SCID mice with established tumors (tumors volume $\geqslant$ 200 mm^3) were randomly divided into three groups and treated with vehicle, 50 mg/kg of compound **24** or vismodegib daily by oral gavage. As shown in Figure 5A, although tumor grew steadily as treated with vehicle, both compound **24** and vismodegib significantly suppressed tumor growth, with 94% and 97% growth inhibition, respectively. Meanwhile, no obvious change was observed in the behavior and body weight of mice during compound **24** treatment (Figure 5B), suggesting that compound **24** exhibited dramatic anti-tumor effects without visible signs of gross toxicity.

To determine whether tumor growth inhibition by compound **24** was due to repressed Hh pathway activity, we harvested tumor tissue after drug treatment and evaluated Hh pathway activation based on Gli1 mRNA expression examined by q-PCR. Compared with vehicle treatment, **24** and vismodegib resulted in 94% and 86% inhibition of Gli1 mRNA expression, respectively, indicating that **24** has comparable inhibitory effects on Hh pathway activation with vismodegib (Figure 5C).

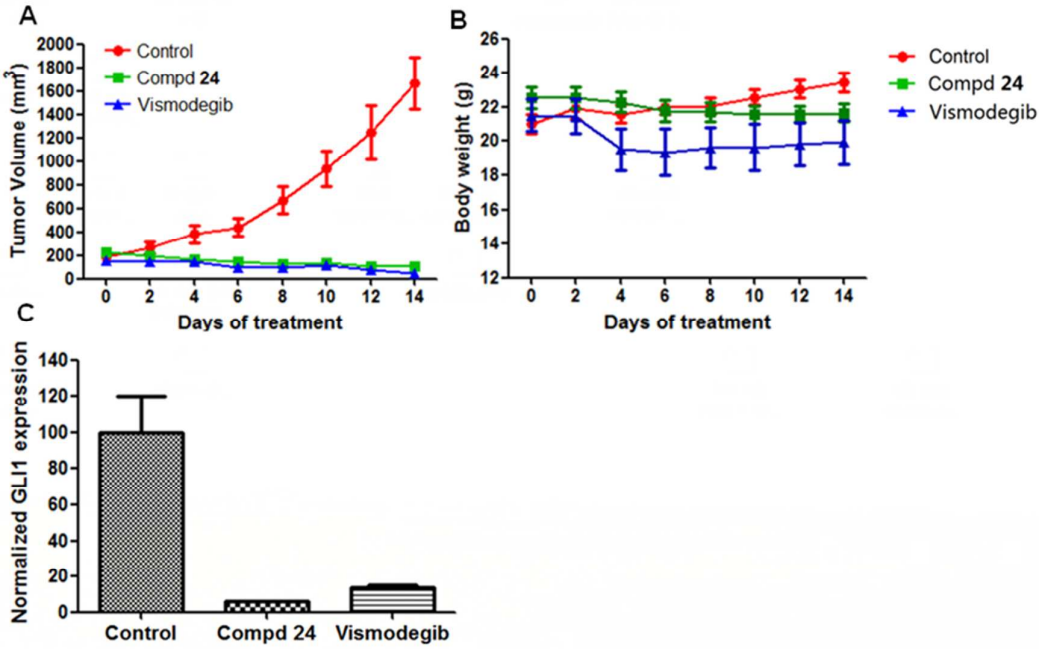

Figure 5. Comparison of preclinical efficacy of compound **24** and vismodegib (p.o., 50 mg/kg) on *Ptch1*$^{+/-}$ medulloblastoma allograft in SCID mice

To further confirm the anti-tumor effects of compound **24**, we tested compound **24** in medulloblastoma of Math1-cre:SmoM2 mice[74,75], a mouse model harboring constitutively active Smo (*SmoM2*) allele, which was conditionally activated by Cre recombinase in granule cell precursors. The Math1-cre:SmoM2 mice have a heavy tumor burden in cerebellum, the mouse was very sick and hunched up within one month. Treatment with compound **24** for 2 weeks significantly reduced the tumor volume in cerebellum, and apparently improved the physical conditions of the mouse (Figure 6). The results above indicate that compound **24** has significant anti-tumor effects without signs of toxicity.

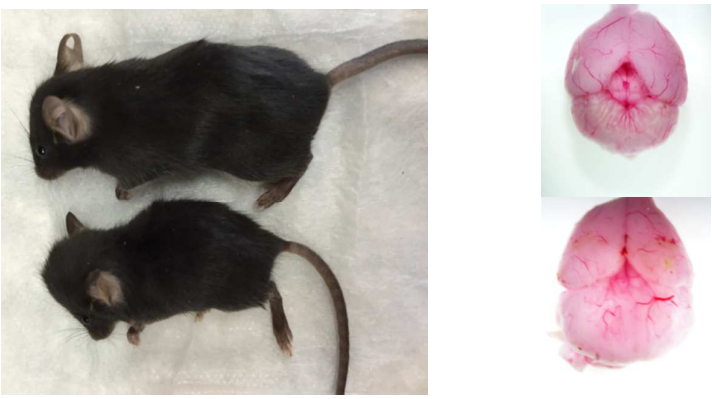

Figure 6. Treatment of Math1cre/SmoM2 medulloblastoma mouse with 100 mg/kg of compound **24** by oral administration for 2 weeks (start treatment when the mice are 2 weeks old, upper panel) and control (lower panel).

CONCLUSIONS

Through a scaffold hopping strategy, we have identified a series of novel tetrahydropyrido[4,3-*d*]pyrimidine derivatives, which exhibited effective inhibition of Hh signaling. Among them, compound **24** is three times more potent than vismodegib in the NIH3T3-GRE-Luc reporter gene assay. Compound **24** has lower melting point and much greater solubility compared with vismodegib, resulting in linear PK profiles when dosed orally at 10, 30, and 100 mg/kg in rats. In addition, compound **24** showed excellent PK profiles with a 72% oral bioavailability in beagle dogs. Compound **24** demonstrated overall favorable in vitro safety profiles with respect to CYP isoform and hERG inhibition. Finally, compound **24** led to significant regression of subcutaneous tumor generated by primary Ptch1-deficient medulloblastoma cells in SCID mouse. In conclusion, tetrahydropyrido[4,3-*d*]pyrimidine derivatives represent a novel set of Smo inhibitors that could potentially be utilized to treat medulloblastoma and other Hh pathway related malignancies.

EXPERIMENTAL METHODS

Chemistry. Full experimental details, characterization of intermediates and final compounds can be found in the Supporting Information.

In vitro biological assays. NIH3T3-GRE-Luc reporter gene assay and BODIPY-Cyclopamine binding assay were performed aspreviously described.[52] The detailed experimental procedures can be found in the Supporting Information.

Solubility. Solubility at pH = 6.5 and PH = 1 were measured as previouslydescribed.[52] The detailed experimental procedures can be found in the Supporting Information.

Permeability. Caco-2 permeability test was performed according to the methodology described in the literature.[76]

CYP inhibitory potency. CYP inhibitory potency was evaluated as previously reported.[66] The detailed experimental procedures can be found in the Supporting Information.

hERG assays.[77] Compound **24** was evaluated for block of the hERG K channel using CHO cells stably expressing the hERG gene and the QPatch platform (Sophion, Ballerup, Denmark). K tail currents were measured at −50 mV following a 500 ms depolarization to +20 mV from a holding voltage of −80 mV. The external solution contained 4 mM K^+, 1 mM Mg^{2+},and 2 mM Ca^{2+}. Compound effects were quantified 4 min after application to the cells. Pulses were elicited every 20 s.

In vivo mouse PK in-life phase. Male ICR mice received either a single intravenous (bolus) injection or single oral administration (by gavage) of compound **24** (HCl salt). Doses of 2 mg/kg (i.v.) and 10 mg/kg (p.o.) were given as solutions in saline. Blood samples were collected by heart puncture from n = 3 animals per route of administration after 0.08 (i.v. only), 0.25, 0.5, 1, 2, 4, 6 (p.o. only), 8 h, and 24 h and were further processed to obtain plasma.

In vivo rat PK in-life phase. Male Sprague-Dawley rats (body weight, 220-250 g) received either a

single intravenous (bolus) injection or a single oral administration (by gavage) of the compound (HCl salts). Doses of 2 mg/kg (per compound, i.v.), 10 mg/kg for compound **16** (p.o.) and 10/30/100 mg/kg for compound **24** (p.o.) were given as solutions in saline. Consecutive blood samples were collected via retro-orbital bleeding from n = 3 animals per route of administration after 0.08 (i.v. only), 0.25 (p.o. only), 0.5, 1, 2, 4, 8 h, and 24 h and were further processed to obtain plasma.

In vivo dog PK in-life phase. Female Beagle dogs received either a single intravenous (bolus) injection or an oral administration (by gavage) of compound **24** (HCl salt). Doses of 1 and 5 mg/kg were given intravenously and per orally as a solution in saline. Consecutive blood samples were taken by puncture of the vena cephalica from n = 3 animals per route of administration after 0.08 (i.v. only), 0.25, 0.5, 1, 2, 4, 8, and 24 h and were further processed to obtain plasma.

Bioanalysis. The concentrations of compound in plasma were analyzed by a LC-MS/MS system as previously reported.[55]

14-Day repeat-dose mouse toxicity study. ICR mice were randomly assigned to 4 groups by using a simple randomization procedure based on body weight and sex. 5 male and 5 female animals were assigned to each group. Animals in group 1 to 4 were administered (p.o.) with compound 24 (HCl salt) at 0, 100, 250, and 500 mg/kg/day as solutions in saline (10 mL/kg/day) for consecutive 14 days, once daily. Cage side observation was given to all animals twice daily. A detailed physical examination was conducted for all animals once daily during the dosing periods. Body weights were measured and recorded once prior to group assignment, and once on Day 1, Day 4, Day 7, Day10, and Day13 during dosing period. Food consumption was measured on Day 1, Day 4, Day 7, Day10, and Day13. On the necropsy days of the dosing period, the survival animals were transferred to pathology department for necropsy, they were euthanized by carbon dioxide inhalation and the organs (brain, adrenal gland, heart,

kidney, liver, spleen, testis, and thymus) were weighed.

Subcutaneous tumor allograft. Experiments were performed in female *CB17 SCID* mice between 8 and 12 weeks of age. *CB17 SCID* mice were bred in the Fox Chase Cancer Center Laboratory Animal Facility (LAF). All animals were maintained in the LAF at Fox Chase Cancer Center and all experiments were performed in accordance with procedures approved by the Fox Chase Cancer Center Animal Care and Use Committee. Tumor cells from *Ptch1*$^{+/-}$ mouse medulloblastoma were resuspended in reduced growth factor matrigel (BD 356231) with ice-cold PBS in 80:20 ratio, 2 x 10^6 cells in 50 μL matrigel were injected into the right flank area of the animals. The mice were randomly divided into 3 groups consisting of 6 mice each when the tumor volume reach around 200 mm^3, the mice were administrated with vehicle control (MCT solution: 0.5% Methyl Cellulose with 0.2% Tween 80 in distilled water), 50 mg/kg Vismodegib (dissolved in MCT solution) and 50 mg/kg compound **24** (dissolved in distilled water) daily by oral gavage for two weeks. The tumor volume were calculated using the formula $V = (W^2 \times L)/2$, where V is tumor volume, W is tumor width, L is tumor length.

q-PCR for Gli1 mRNA expression. Tumor tissues were homogenized and total RNA was isolated using Trizol reagent (Sigma) following the manufacturer's instructions. cDNA was synthesized using oligo(dT) and Superscript II reverse transcriptase (Invitrogen). Quantitative PCR reactions were performed in triplicate using iQ SYBR Green Supermix (Bio-Rad) and the Bio-Rad iQ5 Multicolor Real-Time PCR Detection System. Gli1 expression was normalized to Actin. Primer sequences are available upon request.

ASSOCIATED CONTENT

Supporting Information

In vitro biological assays S2, Solubility test S3, Evaluation of CYP inhibitory potency S3, Results of 14-Day repeat-dose mouse toxicity study S4, Chemistry S5, Spectral Data and spectra. The Supporting Information is available free of charge on the ACS Publications website.

AUTHOR INFORMATION

Corresponding Author

*(X.Z.) E-mail: xiaohuzhang@suda.edu.cn; Tel.: +86 512 65880380; fax: +86 512 65880380.

*(L.L.) E-mail: lusong.luo@beigene.com.

*(Z.Y.) E-mail: Zeng-Jie.Yang@fccc.edu.

Author Contributions

[#]W.L., Y.L., and H.M. contributed equallyto this paper.

Notes

The authors declare no competing financial interest.

ACKNOWLEDGMENTS

This work was supported by National Natural Science Foundation of China (Grant No. 81473090, 81473278, 81572724, 21502133,81273372), Natural Science Foundation of Jiangsu Province (BK20140313), BM2013003, and PAPD (A Project Funded by the Priority Academic Program Development of Jiangsu Higher Education Institutions).

ABBREVIATIONS USED

AUC, area under the plasma time-concentration curve; CL, clearance; CYP, cytochrome P450; *m*-CPBA, *m*-chloroperoxybenzoic acid; DIPEA, *N*,*N*-diisopropylethylamine; DMF, *N*,*N*-dimethylformamide; DMF-DMA, *N*,*N*-dimethylformamide dimethyl acetal; DMSO, dimethyl

sulfoxide; GPCR, G protein-coupled receptor; hERG, the human ether-a-go-go related gene; Hh, hedgehog; HPLC, high performance liquid chromatography; i.v., intraveneous administration; LAF, Laboratory Animal Facility; LDA, lithium diisopropylamide; MCT solution, 0.5% Methyl Cellulose with 0.2% Tween 80 in distilled water; N-G-L, NIH3T3-GRE-Luc reporter gene assay; PBS, phosphate buffer saline; PK, pharmacokinetics; p.o., per oral administration; Ptch, Patched; q-PCR, quantitative real-time polymerase chain reaction; SAR, structure–activity relationship; SCID, severe combined immunodeficiency; SD mouse, Sprague-Dawley mouse; SEM, standard error measurement; Smo, Smoothened; SMO-BCB, BODIPY-Cyclopamine binding assay; SP, standard precision; SUFU, suppressor of fused; THF, tetrahydrofuran; XP, extra precision.

REFERENCES

(1) Crawford, J. R., MacDonald, T. J., and Packer, R. J. (2007) Medulloblastoma in childhood: new biological advances, *Lancet Neurol. 6*, 1073-1085.

(2) Gilbertson, R. J. (2004) Medulloblastoma: signalling a change in treatment, *Lancet Oncol. 5*, 209-218.

(3) Varjosalo, M., and Taipale, J. (2008) Hedgehog: functions and mechanisms, *Genes Dev. 22*, 2454-2472.

(4) Jiang, J., and Hui, C. C. (2008) Hedgehog signaling in development and cancer, *Dev. Cell 15*, 801-812.

(5) Ingham, P. W. (1998) The patched gene in development and cancer, *Curr. Opin. Genet. Dev. 8*, 88-94.

(6) Xie, J., Murone, M., Luoh, S. M., Ryan, A., Gu, Q., Zhang, C., Bonifas, J. M., Lam, C. W., Hynes, M., Goddard, A., Rosenthal, A., Epstein, E. H., Jr., and de Sauvage, F. J. (1998) Activating Smoothened mutations in sporadic basal-cell carcinoma, *Nature 391*, 90-92.

(7) Scales, S. J., and de Sauvage, F. J. (2009) Mechanisms of Hedgehog pathway activation in cancer and implications for therapy, *Trends Pharmacol. Sci. 30*, 303-312.

(8) Yang, L., Xie, G., Fan, Q., and Xie, J. (2010) Activation of the hedgehog-signaling pathway in human cancer and the clinical implications, *Oncogene 29*, 469-481.

(9) Ng, J. M., and Curran, T. (2011) The Hedgehog's tale: developing strategies for targeting cancer, *Nat. Rev. Cancer 11*, 493-501.

(10) Peukert, S., and Miller-Moslin, K. (2010) Small-molecule inhibitors of the hedgehog signaling pathway as cancer therapeutics, *ChemMedChem 5*, 500-512.

(11) Li, Y., Maitah, M. Y., Ahmad, A., Kong, D., Bao, B., and Sarkar, F. H. (2012) Targeting the Hedgehog signaling pathway for cancer therapy, *Expert Opin. Ther. Targets 16*, 49-66.

(12) Yun, J. I., Kim, H. R., Park, H., Kim, S. K., and Lee, J. (2012) Small molecule inhibitors of

the hedgehog signaling pathway for the treatment of cancer, *Arch. Pharm. Res.35*, 1317-1333.

(13) Hadden, M. K. (2013) Hedgehog pathway inhibitors: a patent review (2009--present), *Expert Opin. Ther. Pat. 23*, 345-361.

(14) Amakye, D., Jagani, Z., and Dorsch, M. (2013) Unraveling the therapeutic potential of the Hedgehog pathway in cancer, *Nat. Med. 19*, 1410-1422.

(15) Ruat, M., Hoch, L., Faure, H., and Rognan, D. (2014) Targeting of Smoothened for therapeutic gain, *Trends Pharmacol. Sci. 35*, 237-246.

(16) Chen, J. K., Taipale, J., Cooper, M. K., and Beachy, P. A. (2002) Inhibition of Hedgehog signaling by direct binding of cyclopamine to Smoothened, *Genes Dev. 16*, 2743-2748.

(17) Tremblay, M. R., Nevalainen, M., Nair, S. J., Porter, J. R., Castro, A. C., Behnke, M. L., Yu, L. C., Hagel, M., White, K., Faia, K., Grenier, L., Campbell, M. J., Cushing, J., Woodward, C. N., Hoyt, J., Foley, M. A., Read, M. A., Sydor, J. R., Tong, J. K., Palombella, V. J., McGovern, K., and Adams, J. (2008) Semisynthetic cyclopamine analogues as potent and orally bioavailable hedgehog pathway antagonists, *J. Med. Chem. 51*, 6646-6649.

(18) Tremblay, M. R., Lescarbeau, A., Grogan, M. J., Tan, E., Lin, G., Austad, B. C., Yu, L. C., Behnke, M. L., Nair, S. J., Hagel, M., White, K., Conley, J., Manna, J. D., Alvarez-Diez, T. M., Hoyt, J., Woodward, C. N., Sydor, J. R., Pink, M., MacDougall, J., Campbell, M. J., Cushing, J., Ferguson, J., Curtis, M. S., McGovern, K., Read, M. A., Palombella, V. J., Adams, J., and Castro, A. C. (2009) Discovery of a potent and orally active hedgehog pathway antagonist (IPI-926), *J. Med. Chem. 52*, 4400-4418.

(19) Ma, H., Li, H. Q., and Zhang, X. (2013) Cyclopamine, a naturally occurring alkaloid, and its analogues may find wide applications in cancer therapy, *Curr. Top. Med. Chem.13*, 2208-2215.

(20) Infinity Stops Phase 2 Trials of Saridegib in Chondrosarcoma and Myelofibrosis, Infinity Pharmaceuticals press release, January 18, 2012, http://phx.corporate-ir.net/phoenix.zhtml?c=121941&p=irol-newsArticle&ID=1705831&highlight=.

(21) Novartis investigational compound LDE225 met primary endpoint in pivotal trial for patients with advanced basal cell carcinoma, Novartis press release, February 19, 2014, http://www.novartis.com/newsroom/media-releases/en/2014/1762942.shtml.

(22) Pivotal data for Novartis' investigational compound LDE225 show marked tumor responses in advanced basal cell carcinoma, Novartis press release, June 01, 2014, http://www.novartis.com/newsroom/media-releases/en/2014/1789711.shtml.

(23) Miller-Moslin, K., Peukert, S., Jain, R. K., McEwan, M. A., Karki, R., Llamas, L., Yusuff, N., He, F., Li, Y., Sun, Y., Dai, M., Perez, L., Michael, W., Sheng, T., Lei, H., Zhang, R., Williams, J., Bourret, A., Ramamurthy, A., Yuan, J., Guo, R., Matsumoto, M., Vattay, A., Maniara, W., Amaral, A., Dorsch, M., and Kelleher, J. F., 3rd. (2009) 1-amino-4-benzylphthalazines as orally bioavailable smoothened antagonists with antitumor activity, *J. Med. Chem. 52*, 3954-3968.

(24) Mahindroo, N., Punchihewa, C., and Fujii, N. (2009) Hedgehog-Gli signaling pathway inhibitors as anticancer agents, *J. Med. Chem. 52*, 3829-3845.

(25) Robarge, K. D., Brunton, S. A., Castanedo, G. M., Cui, Y., Dina, M. S., Goldsmith, R., Gould, S. E., Guichert, O., Gunzner, J. L., Halladay, J., Jia, W., Khojasteh, C., Koehler, M. F., Kotkow, K., La, H., Lalonde, R. L., Lau, K., Lee, L., Marshall, D., Marsters, J. C., Jr., Murray, L. J., Qian, C., Rubin, L. L., Salphati, L., Stanley, M. S., Stibbard, J. H., Sutherlin, D. P., Ubhayaker,

S., Wang, S., Wong, S., and Xie, M. (2009) GDC-0449-a potent inhibitor of the hedgehog pathway, *Bioorg. Med. Chem. Lett. 19*, 5576-5581.

(26) Lucas, B. S., Aaron, W., An, S., Austin, R. J., Brown, M., Chan, H., Chong, A., Hungate, R., Huang, T., Jiang, B., Johnson, M. G., Kaizerman, J. A., Lee, G., McMinn, D. L., Orf, J., Powers, J. P., Rong, M., Toteva, M. M., Uyeda, C., Wickramasinghe, D., Xu, G., Ye, Q., and Zhong, W. (2010) Design of 1-piperazinyl-4-arylphthalazines as potent Smoothened antagonists, *Bioorg. Med. Chem. Lett. 20*, 3618-3622.

(27) Malancona, S., Altamura, S., Filocamo, G., Kinzel, O., Hernando, J. I., Rowley, M., Scarpelli, R., Steinkuhler, C., and Jones, P. (2011) Identification of MK-5710 ((8aS)-8a-methyl-1,3-dioxo-2-[(1S,2R)-2-phenylcyclopropyl]-N-(1-phenyl-1H-pyrazol -5-yl)hexahydroimid azo[1,5-a]pyrazine-7(1H)-carboxamide), a potent smoothened antagonist for use in Hedgehog pathway dependent malignancies, part 1, *Bioorg. Med. Chem. Lett. 21*, 4422-4428.

(28) Kinzel, O., Alfieri, A., Altamura, S., Brunetti, M., Bufali, S., Colaceci, F., Ferrigno, F., Filocamo, G., Fonsi, M., Gallinari, P., Malancona, S., Hernando, J. I., Monteagudo, E., Orsale, M. V., Palumbi, M. C., Pucci, V., Rowley, M., Sasso, R., Scarpelli, R., Steinkuhler, C., and Jones, P. (2011) Identification of MK-5710 ((8aS)-8a-methyl-1,3-dioxo-2-[(1S,2R)-2-phenylcyclo-propyl]-N-(1-phenyl-1H-pyrazol-5-yl) hexahydro-imidazo[1,5-a]pyrazine-7(1H)-carboxamide), a potent smoothened antagonist for use in Hedgehog pathway dependent malignancies, part 2, *Bioorg. Med. Chem. Lett. 21*, 4429-4435.

(29) Brown, M. L., Aaron, W., Austin, R. J., Chong, A., Huang, T., Jiang, B., Kaizerman, J. A., Lee, G., Lucas, B. S., McMinn, D. L., Orf, J., Rong, M., Toteva, M. M., Xu, G., Ye, Q., Zhong, W., Degraffenreid, M. R., Wickramasinghe, D., Powers, J. P., Hungate, R., and Johnson, M. G. (2011) Discovery of amide replacements that improve activity and metabolic stability of a bis-amide smoothened antagonist hit, *Bioorg. Med. Chem. Lett. 21*, 5206-5209.

(30) Pan, S., Wu, X., Jiang, J., Gao, W., Wan, Y., Cheng, D., Han, D., Liu, J., Englund, N. P., Wang, Y., Peukert, S., Miller-Moslin, K., Yuan, J., Guo, R., Matsumoto, M., Vattay, A., Jiang, Y., Tsao, J., Sun, F., Pferdekamper, A. C., Dodd, S., Tuntland, T., Maniara, W., Kelleher, J. F., 3rd, Yao, Y. M., Warmuth, M., Williams, J., and Dorsch, M. (2010) Discovery of NVP-LDE225, a Potent and Selective Smoothened Antagonist, *ACS Med. Chem. Lett. 1*, 130-134.

(31) Munchhof, M. J., Li, Q., Shavnya, A., Borzillo, G. V., Boyden, T. L., Jones, C. S., LaGreca, S. D., Martinez-Alsina, L., Patel, N., Pelletier, K., Reiter, L. A., Robbins, M. D., and Tkalcevic, G. T. (2012) Discovery of PF-04449913, a Potent and Orally Bioavailable Inhibitor of Smoothened, *ACS Med. Chem. Lett. 3*, 106-111.

(32) Betti, M., Castagnoli, G., Panico, A., Sanna Coccone, S., and Wiedenau, P. (2012) Development of a scalable route to the SMO receptor antagonist SEN794, *Org. Process Res. Dev. 16*, 1739-1745.

(33) Peukert, S., He, F., Dai, M., Zhang, R., Sun, Y., Miller-Moslin, K., McEwan, M., Lagu, B., Wang, K., Yusuff, N., Bourret, A., Ramamurthy, A., Maniara, W., Amaral, A., Vattay, A., Wang, A., Guo, R., Yuan, J., Green, J., Williams, J., Buonamici, S., Kelleher, J. F., 3rd, and Dorsch, M. (2013) Discovery of NVP-LEQ506, a second-generation inhibitor of smoothened, *ChemMedChem 8*, 1261-1265.

(34) Manetti, F., Faure, H., Roudaut, H., Gorojankina, T., Traiffort, E., Schoenfelder, A., Mann, A.,

Solinas, A., Taddei, M., and Ruat, M. (2010) Virtual screening-based discovery and mechanistic characterization of the acylthiourea MRT-10 family as smoothened antagonists, *Mol. Pharmacol. 78*, 658-665.

(35) Solinas, A., Faure, H., Roudaut, H., Traiffort, E., Schoenfelder, A., Mann, A., Manetti, F., Taddei, M., and Ruat, M. (2012) Acylthiourea, acylurea, and acylguanidine derivatives with potent hedgehog inhibiting activity, *J. Med. Chem. 55*, 1559-1571.

(36) Xin, M., Wen, J., Tang, F., Tu, C., Shen, H., and Zhao, X. (2013) The discovery of novel N-(2-pyrimidinylamino) benzamide derivatives as potent hedgehog signaling pathway inhibitors, *Bioorg. Med. Chem. Lett. 23*, 6777-6783.

(37) Hoch, L., Faure, H., Roudaut, H., Schoenfelder, A., Mann, A., Girard, N., Bihannic, L., Ayrault, O., Petricci, E., Taddei, M., Rognan, D., and Ruat, M. (2015) MRT-92 inhibits Hedgehog signaling by blocking overlapping binding sites in the transmembrane domain of the Smoothened receptor, *FASEB J. 29*, 1817-1829.

(38) Curis Announces FDA Approval of Erivedge(TM) (vismodegib) Capsule as First Treatment for Advanced Basal Cell Carcinoma, Curis Pharmaceuticals press release, January 30, 2012, http://investors.curis.com/releasedetail.cfm?ReleaseID=643756.

(39) Yauch, R. L., Dijkgraaf, G. J., Alicke, B., Januario, T., Ahn, C. P., Holcomb, T., Pujara, K., Stinson, J., Callahan, C. A., Tang, T., Bazan, J. F., Kan, Z., Seshagiri, S., Hann, C. L., Gould, S. E., Low, J. A., Rudin, C. M., and de Sauvage, F. J. (2009) Smoothened mutation confers resistance to a Hedgehog pathway inhibitor in medulloblastoma, *Science 326*, 572-574.

(40) Sharpe, H. J., Pau, G., Dijkgraaf, G. J., Basset-Seguin, N., Modrusan, Z., Januario, T., Tsui, V., Durham, A. B., Dlugosz, A. A., Haverty, P. M., Bourgon, R., Tang, J. Y., Sarin, K. Y., Dirix, L., Fisher, D. C., Rudin, C. M., Sofen, H., Migden, M. R., Yauch, R. L., and de Sauvage, F. J. (2015) Genomic analysis of smoothened inhibitor resistance in basal cell carcinoma, *Cancer Cell 27*, 327-341.

(41) Atwood, S. X., Sarin, K. Y., Whitson, R. J., Li, J. R., Kim, G., Rezaee, M., Ally, M. S., Kim, J., Yao, C., Chang, A. L., Oro, A. E., and Tang, J. Y. (2015) Smoothened variants explain the majority of drug resistance in basal cell carcinoma, *Cancer Cell 27*, 342-353.

(42) FDA approves Novartis drug Odomzo® (sonidegib) for locally advanced basal cell carcinoma (laBCC), a form of skin cancer, Novartis press release, February 19, 2014, https://www.novartis.com/news/media-releases/fda-approves-novartis-drug-odomzo%C2%AE-sonidegib-locally-advanced-basal-cell.

(43) Byrne, E. F., Sircar, R., Miller, P. S., Hedger, G., Luchetti, G., Nachtergaele, S., Tully, M. D., Mydock-McGrane, L., Covey, D. F., Rambo, R. P., Sansom, M. S., Newstead, S., Rohatgi, R., and Siebold, C. (2016) Structural basis of Smoothened regulation by its extracellular domains, *Nature 535*, 517-522.

(44) Sharpe, H. J., Wang, W., Hannoush, R. N., and de Sauvage, F. J. (2015) Regulation of the oncoprotein Smoothened by small molecules, *Nat. Chem. Biol. 11*, 246-255.

(45) Wang, C., Wu, H., Evron, T., Vardy, E., Han, G. W., Huang, X. P., Hufeisen, S. J., Mangano, T. J., Urban, D. J., Katritch, V., Cherezov, V., Caron, M. G., Roth, B. L., and Stevens, R. C. (2014) Structural basis for Smoothened receptor modulation and chemoresistance to anticancer drugs, *Nat. commun. 5*, 4355.

(46) Weierstall, U., James, D., Wang, C., White, T. A., Wang, D., Liu, W., Spence, J. C., Bruce Doak, R., Nelson, G., Fromme, P., Fromme, R., Grotjohann, I., Kupitz, C., Zatsepin, N. A.,

Liu, H., Basu, S., Wacker, D., Han, G. W., Katritch, V., Boutet, S., Messerschmidt, M., Williams, G. J., Koglin, J. E., Marvin Seibert, M., Klinker, M., Gati, C., Shoeman, R. L., Barty, A., Chapman, H. N., Kirian, R. A., Beyerlein, K. R., Stevens, R. C., Li, D., Shah, S. T., Howe, N., Caffrey, M., and Cherezov, V. (2014) Lipidic cubic phase injector facilitates membrane protein serial femtosecond crystallography, *Nat. commun. 5*, 3309.

(47) Wang, C., Wu, H., Katritch, V., Han, G. W., Huang, X. P., Liu, W., Siu, F. Y., Roth, B. L., Cherezov, V., and Stevens, R. C. (2013) Structure of the human smoothened receptor bound to an antitumour agent, *Nature 497*, 338-343.

(48) Zhang, X., Tellew, J. E., Luo, Z., Moorjani, M., Lin, E., Lanier, M. C., Chen, Y., Williams, J. P., Saunders, J., Lechner, S. M., Markison, S., Joswig, T., Petroski, R., Piercey, J., Kargo, W., Malany, S., Santos, M., Gross, R. S., Wen, J., Jalali, K., O'Brien, Z., Stotz, C. E., Crespo, M. I., Diaz, J. L., and Slee, D. H. (2008) Lead optimization of 4-acetylamino-2-(3,5-dimethylpyrazol-1-yl)-6-pyridylpyrimidines as A2A adenosine receptor antagonists for the treatment of Parkinson's disease, *J. Med. Chem. 51*, 7099-7110.

(49) Lanier, M. C., Moorjani, M., Luo, Z., Chen, Y., Lin, E., Tellew, J. E., Zhang, X., Williams, J. P., Gross, R. S., Lechner, S. M., Markison, S., Joswig, T., Kargo, W., Piercey, J., Santos, M., Malany, S., Zhao, M., Petroski, R., Crespo, M. I., Diaz, J. L., Saunders, J., Wen, J., O'Brien, Z., Jalali, K., Madan, A., and Slee, D. H. (2009) N-[6-amino-2-(heteroaryl)pyrimidin-4-yl]acetamides as A2A receptor antagonists with improved drug like properties and in vivo efficacy, *J. Med. Chem. 52*, 709-717.

(50) Lovering, F., Bikker, J., and Humblet, C. (2009) Escape from flatland: increasing saturation as an approach to improving clinical success, *J. Med. Chem. 52*, 6752-6756.

(51) Yang, Y., Engkvist, O., Llinas, A., and Chen, H. (2012) Beyond size, ionization state, and lipophilicity: influence of molecular topology on absorption, distribution, metabolism, excretion, and toxicity for druglike compounds, *J. Med. Chem. 55*, 3667-3677.

(52) Rohner, A., Spilker, M. E., Lam, J. L., Pascual, B., Bartkowski, D., Li, Q. J., Yang, A. H., Stevens, G., Xu, M., Wells, P. A., Planken, S., Nair, S., and Sun, S. (2012) Effective targeting of Hedgehog signaling in a medulloblastoma model with PF-5274857, a potent and selective Smoothened antagonist that penetrates the blood-brain barrier, *Mol. Cancer Ther. 11*, 57-65.

(53) Lipinski, C. A., Lombardo, F., Dominy, B. W., and Feeney, P. J. (2001) Experimental and computational approaches to estimate solubility and permeability in drug discovery and development settings, *Adv. Drug Deliv. Rev. 46*, 3-26.

(54) Lu, W., Geng, D., Sun, Z., Yang, Z., Ma, H., Zheng, J., and Zhang, X. (2014) Scaffold hopping approach to a new series of smoothened antagonists, *Bioorg. Med. Chem. Lett. 24*, 2300-2304.

(55) Ma, H., Lu, W., Sun, Z., Luo, L., Geng, D., Yang, Z., Li, E., Zheng, J., Wang, M., Zhang, H., Yang, S., and Zhang, X. (2015) Design, synthesis, and structure--activity-relationship of tetrahydrothiazolopyridine derivatives as potent smoothened antagonists, *Eur. J. Med. Chem. 89*, 721-732.

(56) Schrödinger, version 9.0, Schrödinger, LLC., New York, 2009, http://www.schrodinger.com.

(57) Tian, S., Sun, H., Pan, P., Li, D., Zhen, X., Li, Y., and Hou, T. (2014) Assessing an ensemble docking-based virtual screening strategy for kinase targets by considering protein flexibility, *J Chem. Inf. Model 54*, 2664-2679.

(58) Discovery Studio 2.5 Guide, Accelrys Inc., San Diego, 2009, http://www.accelrys.com.

(59) Voisin, A. S., Bouillon, A., Lancelot, J.-C., and Rault, S. (2005) Efficient synthesis of

halohydroxypyridines by hydroxydeboronation, *Tetrahedron 61*, 1417-1421.

(60) Yang, Z., Ma, H., Sun, Z., Luo, L., Tian, S., Zheng, J., and Zhang, X. (2015) Discovery of a 6-(pyridin-3-yl)benzo[d]thiazole template for optimization of hedgehog and PI3K/AKT/mTOR dual inhibitors, *Bioorg. Med. Chem. Lett. 25*, 3665-3670.

(61) Taipale, J., Chen, J. K., Cooper, M. K., Wang, B., Mann, R. K., Milenkovic, L., Scott, M. P., and Beachy, P. A. (2000) Effects of oncogenic mutations in Smoothened and Patched can be reversed by cyclopamine, *Nature 406*, 1005-1009.

(62) Chen, J. K., Taipale, J., Young, K. E., Maiti, T., and Beachy, P. A. (2002) Small molecule modulation of Smoothened activity, *Proc. Natl. Acad. Sci. U. S. A. 99*, 14071-14076.

(63) Stanton, B. Z., Peng, L. F., Maloof, N., Nakai, K., Wang, X., Duffner, J. L., Taveras, K. M., Hyman, J. M., Lee, S. W., Koehler, A. N., Chen, J. K., Fox, J. L., Mandinova, A., and Schreiber, S. L. (2009) A small molecule that binds Hedgehog and blocks its signaling in human cells, *Nat. Chem. Biol. 5*, 154-156.

(64) Petrova, E., Rios-Esteves, J., Ouerfelli, O., Glickman, J. F., and Resh, M. D. (2013) Inhibitors of Hedgehog acyltransferase block Sonic Hedgehog signaling, *Nat. Chem. Biol. 9*, 247-249.

(65) Wang, J., Lu, J., Bond, M. C., Chen, M., Ren, X. R., Lyerly, H. K., Barak, L. S., and Chen, W. (2010) Identification of select glucocorticoids as Smoothened agonists: potential utility for regenerative medicine, *Proc. Natl. Acad. Sci. U. S. A. 107*, 9323-9328.

(66) Wang, J., Mook, R. A., Jr., Lu, J., Gooden, D. M., Ribeiro, A., Guo, A., Barak, L. S., Lyerly, H. K., and Chen, W. (2012) Identification of a novel Smoothened antagonist that potently suppresses Hedgehog signaling, *Bioorg. Med. Chem. 20*, 6751-6757.

(67) Stepan, A. F., Walker, D. P., Bauman, J., Price, D. A., Baillie, T. A., Kalgutkar, A. S., and Aleo, M. D. (2011) Structural alert/reactive metabolite concept as applied in medicinal chemistry to mitigate the risk of idiosyncratic drug toxicity: a perspective based on the critical examination of trends in the top 200 drugs marketed in the United States, *Chem. Res. Toxicol. 24*, 1345-1410.

(68) Argikar, U. A., Mangold, J. B., and Harriman, S. P. (2011) Strategies and chemical design approaches to reduce the potential for formation of reactive metabolic species, *Curr. Top. Med. Chem. 11*, 419-449.

(69) Dong, Y., Li, K., Xu, Z., Ma, H., Zheng, J., Hu, Z., He, S., Wu, Y., Sun, Z., Luo, L., Li, J., Zhang, H., and Zhang, X. (2015) Exploration of the linkage elements of porcupine antagonists led to potent Wnt signaling pathway inhibitors, *Bioorg. Med. Chem. 23*, 6855-6868.

(70) Xu, Z., Li, J., Wu, Y., Sun, Z., Luo, L., Hu, Z., He, S., Zheng, J., Zhang, H., and Zhang, X. (2016) Design, synthesis, and evaluation of potent Wnt signaling inhibitors featuring a fused 3-ring system, *Eur. J. Med. Chem. 108*, 154-165.

(71) Kim, J., Tang, J. Y., Gong, R., Kim, J., Lee, J. J., Clemons, K. V., Chong, C. R., Chang, K. S., Fereshteh, M., Gardner, D., Reya, T., Liu, J. O., Epstein, E. H., Stevens, D. A., and Beachy, P. A. (2010) Itraconazole, a commonly used antifungal that inhibits Hedgehog pathway activity and cancer growth, *Cancer Cell 17*, 388-399.

(72) Kim, J., Aftab, B. T., Tang, J. Y., Kim, D., Lee, A. H., Rezaee, M., Kim, J., Chen, B., King, E. M., Borodovsky, A., Riggins, G. J., Epstein, E. H., Jr., Beachy, P. A., and Rudin, C. M. (2013) Itraconazole and arsenic trioxide inhibit Hedgehog pathway activation and tumor growth associated with acquired resistance to smoothened antagonists, *Cancer Cell 23*, 23-34.

(73) Li, P., Lee, E. H., Du, F., Gordon, R. E., Yuelling, L. W., Liu, Y., Ng, J. M., Zhang, H., Wu, J.,

Korshunov, A., Pfister, S. M., Curran, T., and Yang, Z. J. (2016) Nestin Mediates Hedgehog Pathway Tumorigenesis, *Cancer Res. 76*, 5573-5583.

(74) Xie, J., Murone, M., Luoh, S. M., Ryan, A., Gu, Q., Zhang, C., Bonifas, J. M., Lam, C. W., Hynes, M., Goddard, A., Rosenthal, A., Epstein, E. H., Jr., and de Sauvage, F. J. (1998) Activating Smoothened mutations in sporadic basal-cell carcinoma, *Nature 391*, 90-92.

(75) Jeong, J., Mao, J., Tenzen, T., Kottmann, A. H., and McMahon, A. P. (2004) Hedgehog signaling in the neural crest cells regulates the patterning and growth of facial primordia, *Genes Dev. 18*, 937-951.

(76) Bera, R., Kundu, A., Sen, T., Adhikari, D., and Karmakar, S. (2016) In Vitro Metabolic Stability and Permeability of Gymnemagenin and Its In Vivo Pharmacokinetic Correlation in Rats - A Pilot Study, *Planta Med. 82*, 544-550.

(77) Kutchinsky, J., Friis, S., Asmild, M., Taboryski, R., Pedersen, S., Vestergaard, R. K., Jacobsen, R. B., Krzywkowski, K., Schroder, R. L., Ljungstrom, T., Helix, N., Sorensen, C. B., Bech, M., and Willumsen, N. J. (2003) Characterization of potassium channel modulators with QPatch automated patch-clamp technology: system characteristics and performance, *Assay Drug Dev. Technol. 1*, 685-693.

For Table of Contents Use Only

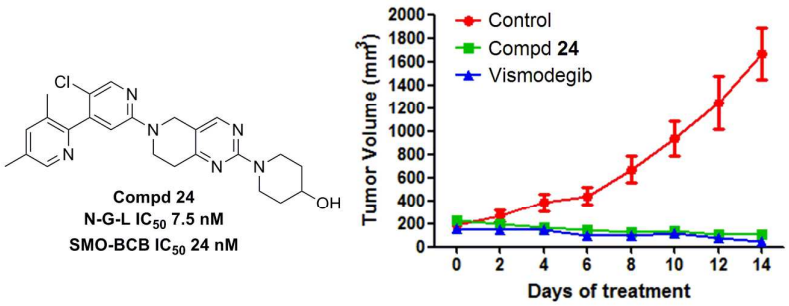

Design, Synthesis, and Structure-Activity-Relationship of Tetrahydropyrido[4,3-d]pyrimidine Derivatives as Potent Smoothened Antagonists with in Vivo Activity

Wenfeng Lu,[†,#] Yongqiang Liu,[‡,#] Haikuo Ma,[†,#] Jiyue Zheng,[†] Sheng Tian,[†] Zhijian Sun,[§] Lusong Luo,*[,§] Jiajun Li,[†] Hongjian Zhang,[†] Zeng-Jie Yang,*[,†,‡] and Xiaohu Zhang*[,†]

[†] Jiangsu Key Laboratory of Translational Research and Therapy for Neuro-Psychiatric-Diseases and College of Pharmaceutical Sciences, Soochow University, Suzhou, Jiangsu 215021, P. R. China

[‡] Cancer Biology Program, Fox Chase Cancer Center, Temple University Health System, Philadelphia, Pennsylvania, USA.

[§] BeiGene (Beijing) Co., Ltd., No. 30 Science Park Road, Zhongguancun Life Science Park, Beijing 102206, P.R.China

[#] W.L., Y.L., H.M. contributed equally to this paper.